

**A universal  
evapotranspiration  
model**

F. M. Anayah and  
J. J. Kaluarachchi

This discussion paper is/has been under review for the journal Hydrology and Earth System Sciences (HESS). Please refer to the corresponding final paper in HESS if available.

# Improving the complementary methods to estimate evapotranspiration under diverse climatic and physical conditions

F. M. Anayah<sup>1</sup> and J. J. Kaluarachchi<sup>2</sup>

<sup>1</sup>Utah Water Research Laboratory, Utah State University, Logan, UT 84322-8200, USA

<sup>2</sup>College of Engineering, Utah State University, Logan, UT 84322-4100, USA

Received: 23 October 2013 – Accepted: 30 October 2013 – Published: 12 November 2013

Correspondence to: F. M. Anayah (fathi.anayah@aggiemail.usu.edu)  
and J. J. Kaluarachchi (jkalu@engineering.usu.edu)

Published by Copernicus Publications on behalf of the European Geosciences Union.

Title Page

Abstract

Introduction

Conclusions

References

Tables

Figures



Back

Close

Full Screen / Esc

Printer-friendly Version

Interactive Discussion

## Abstract

Reliable estimation of evapotranspiration (ET) is important for the purpose of water resources planning and management. Complementary methods, including Complementary Relationship Areal Evapotranspiration (CRAE), Advection–Aridity (AA) and Granger and Gray (GG), have been used to estimate ET because these methods are simple and practical in estimating regional ET using meteorological data only. However, prior studies have found limitations in these methods especially in contrasting climates. This study aims to develop a calibration-free universal model using the complementary relationships to compute regional ET in contrasting climatic and physical conditions with meteorological data only. The proposed methodology consists of a systematic sensitivity analysis using the existing complementary methods. This work used 34 global FLUXNET sites where eddy covariance (EC) fluxes of ET are available for validation. A total of 33 alternative model variations from the original complementary methods were proposed. Further analysis using statistical methods and simplified climatic class definitions produced one distinctly improved GG-model based alternative. The proposed model produced a single-step ET formulation with results equal or better than the recent studies using data-intensive, classical methods. Average root mean square error (RMSE), mean absolute bias (BIAS) and  $R^2$  values across 34 global sites were  $20.57 \text{ mm month}^{-1}$ ,  $10.55 \text{ mm month}^{-1}$  and 0.64, respectively. The proposed model showed a step forward toward predicting ET in large river basins with limited data and requiring no calibration.

## 1 Introduction

A reliable estimate of ET in river basins is important for the purpose of water resources planning and management. ET represents a significant portion of rainfall in the water balance especially in semi-arid regions where most rainfall is typically lost as ET (FAO, 1989). Therefore, the uncertainty in estimating ET can lead to the inaccurate prediction

**HESSD**

10, 13595–13634, 2013

### A universal evapotranspiration model

F. M. Anayah and  
J. J. Kaluarachchi

Title Page

Abstract

Introduction

Conclusions

References

Tables

Figures

⏪

⏩

◀

▶

Back

Close

Full Screen / Esc

Printer-friendly Version

Interactive Discussion





ent terms. Still the complementary methods offer a distinct advantage over the classical methods given the simplicity, ready availability of required data and the ability to estimate total water loss as opposed to crop ET only.

Any improvements to the complementary methods cannot be conducted without the use of actual ET measurements. As a part of this study, it is important to use measured ET data for model validation. Currently, ET fluxes are directly measured using the eddy covariance (EC) method that uses surface energy fluxes for weather forecasting and hydrologic modeling. These fluxes include sensible heat ( $H$ ) and latent heat (LE) fluxes. Compared to other methods such as lysimeters, an EC system produces minimal physical disturbance to the surrounding environment and captures the areal fluxes within the footprint area (Luo et al., 2010). Most importantly, EC data are freely accessible worldwide, for example, FLUXNET (<http://fluxnet.ornl.gov/>) which is a global network of micrometeorological sites that use the EC methods to measure land-atmosphere exchange of carbon dioxide, water vapor and energy fluxes (Baldocchi et al., 2001). FLUXNET comprises of free-access regional networks such as AmeriFlux, AsiaFlux, EuroFlux and CarboAfrica. Given the task of finding a large set of global data with different climatic conditions and physical conditions, this study used the FLUXNET sites similar to many other studies (Castellvi and Snyder, 2010; Huntington et al., 2011).

The major limitation of the EC method is the lack of energy balance closure (i.e.,  $H + LE \neq R_n - G_{soil}$  where  $R_n$  is net radiation and  $G_{soil}$  is soil heat flux) that causes underestimation of ET (Wilson et al., 2002). Twine et al. (2000) and Wang et al. (2008) showed that underestimation of ET can be as high as 15%, however, others, Castellvi et al. (2008), Huntington et al. (2011) and Wilson et al. (2002), found lower percentages within measurement uncertainty that can be < 5%. These studies showed that the impact of energy imbalance in the EC method may not be significant as thought earlier (Castellvi and Snyder, 2010). Hence, the EC method is still attractive and served as the standard method for direct measurement of ET fluxes (Castellvi et al., 2008; Luo et al., 2010).

## A universal evapotranspiration model

F. M. Anayah and  
J. J. Kaluarachchi

[Title Page](#)[Abstract](#)[Introduction](#)[Conclusions](#)[References](#)[Tables](#)[Figures](#)[⏪](#)[⏩](#)[◀](#)[▶](#)[Back](#)[Close](#)[Full Screen / Esc](#)[Printer-friendly Version](#)[Interactive Discussion](#)



## A universal evapotranspiration model

F. M. Anayah and  
J. J. Kaluarachchi

Title Page

Abstract

Introduction

Conclusions

References

Tables

Figures

⏪

⏩

◀

▶

Back

Close

Full Screen / Esc

Printer-friendly Version

Interactive Discussion

ET that would occur if the soil-plant surface is wet enough so that ET could approach its potential value, ETP (Granger, 1989). The development of the complementary relationships is discussed by Brutsaert and Stricker (1979), Granger and Gray (1989), Lhomme and Guillon (2006), McMahon et al. (2013), Morton (1983) and Pettijohn and Salvucci (2009). The three definitions of ET are related as

$$ET = 2ETW - ETP \quad (1)$$

where ET, ETW and ETP are in  $\text{mm month}^{-1}$ . Equation (1) which is the Bouchet original expression indicates that an increase in ET is accompanied by an equivalent decrease of ETP, i.e.,  $\delta ET = -\delta ETP$ . In other words, as the surface dries, actual ET decreases causing a reduction in humidity and an increase in temperature of the surrounding air, and as a result ETP will increase. Once ETP and ETW are estimated, ET is subsequently derived.

## 2.2 CRAE method

ETP is estimated by solving the energy balance and vapor transfer equations iteratively (Morton, 1983). ETP is calculated by solving for the equilibrium temperature ( $T_P$  in  $^{\circ}\text{C}$ ) at which the energy balance and vapor transfer equations for a moist surface are equivalent. The procedure describing the iterative solution is given by Morton (1983, Appendix C). The energy balance equation to estimate ETP is given as

$$ETP = R_T - \lambda f_T (T_P - T) \quad (2)$$

where  $R_T$  is the net radiation for soil-plant surfaces ( $\text{mm month}^{-1}$ ) at air temperature  $T$  ( $^{\circ}\text{C}$ ),  $\lambda$  is the heat transfer coefficient ( $\text{mbar}^{\circ}\text{C}^{-1}$ ) and  $f_T$  is the vapor transfer coefficient ( $\text{mm month}^{-1} \text{mbar}^{-1}$ ). To estimate ETW in Eq. (4), the net radiation for soil-plant surfaces at  $T_P$  ( $R_{TP}$ ) is first computed using Eq. (3).

$$R_{TP} = ETP + \gamma f_T (T_P - T) \quad (3)$$

$$ETW = b_1 + b_2 (1 + \gamma / \Delta_P)^{-1} R_{TP} \quad (4)$$

where  $\gamma$  is the psychrometric constant ( $\text{mbar}^\circ\text{C}^{-1}$ ),  $b_1$  is a constant representing advection energy,  $b_2$  is a constant and  $\Delta_p$  is the rate of change of saturation vapor pressure with  $T$  at  $T_p$  ( $\text{mbar}^\circ\text{C}^{-1}$ ). Constants  $b_1$  and  $b_2$  were calibrated using climatic data from arid regions in North America and Africa (Morton, 1983). ETP from Eq. (2) and ETW from Eq. (4) are used in Eq. (1) to calculate ET of the CRAE method.

### 2.3 AA method

In the AA method, Penman (1948) equation ( $\text{ET}_{\text{PEN}}$ ) is used to estimate ETP as shown in Eqs. (5) and (6).

$$\text{ET}_{\text{PEN}} = \frac{\Delta}{\gamma + \Delta} (R_n - G_{\text{soil}}) + \frac{\gamma}{\gamma + \Delta} E_a \quad (5)$$

$$E_a = 10.6 \times (\beta + 0.54U)(e_s - e_a) \quad (6)$$

where  $\Delta$  is the rate of change of saturation vapor pressure with  $T$  ( $\text{mbar}^\circ\text{C}^{-1}$ ),  $R_n$  is the net radiation ( $\text{mm month}^{-1}$ ),  $G_{\text{soil}}$  is the soil heat flux ( $\text{mm month}^{-1}$ ),  $E_a$  is the drying power of air ( $\text{mm month}^{-1}$ ),  $\beta$  is a constant and usually equals to 1.  $U$  is the wind speed at 2 m above ground level ( $\text{m s}^{-1}$ ),  $e_s$  is the saturation vapor pressure at  $T$  (mm Hg) and  $e_a$  is the vapor pressure of air (mm Hg). In the wind formulation of Penman (1956),  $\beta$  was updated to 0.5. Although both wind function formulae (when  $\beta = 1$  or 0.5) are widely used in hydrology, Penman preferred  $\beta$  of 1 (see Brutsaert and Stricker, 1979; McMahon et al., 2013). Brutsaert and Stricker (1979) mentioned that their method is insensitive to the wind function. The first term of Eq. (5) is called the equilibrium ET and the second is the aerodynamic ET that is generated by large scale advection effects. When advection is minimal, the interactions of atmosphere with the soil-plant system will be completely developed and an equilibrium condition is approached (Brutsaert and Stricker, 1979).

## A universal evapotranspiration model

F. M. Anayah and  
J. J. Kaluarachchi

Title Page

Abstract

Introduction

Conclusions

References

Tables

Figures

⏪

⏩

◀

▶

Back

Close

Full Screen / Esc

Printer-friendly Version

Interactive Discussion



ETW of the AA method is calculated using  $ET_{PT}$  of Priestley and Taylor (1972) in which minimal advection is assumed and given by Eq. (7).

$$ET_{PT} = \alpha \frac{\Delta}{\gamma + \Delta} (R_n - G_{soil}) \quad (7)$$

where  $\alpha$  is a coefficient that typically equals to 1.26 or 1.28 (Priestley and Taylor, 1972).

The AA method in this study used  $\alpha$  of 1.28 and  $\beta$  of 1. ETP from Eq. (5) and ETW from Eq. (7) are used in Eq. (1) to calculate ET of the AA method.

## 2.4 GG Method

The complementary relationship given in Eq. (1) is primarily used by the CRAE and AA methods. In the GG method, Granger and Gray (1989) used a modified version as shown in Eq. (8).

$$ET = (1 + \frac{\gamma}{\Delta})ETW - \frac{\gamma}{\Delta}ETP \quad (8)$$

Equation (8) is reduced to Eq. (1) only when  $\gamma = \Delta$ . In this method, two new concepts were proposed and empirically correlated together; relative drying power ( $D$ ) and relative evaporation ( $G$ ) shown in Eqs. (9) and (10), respectively.

$$D = \frac{E_a}{E_a + (R_n - G_{soil})} \quad (9)$$

$$G = \frac{ET}{ETP} \quad (10)$$

where  $D$  indicates the surface dryness, i.e.,  $D$  becomes larger as the surface becomes drier.  $G$  is the ET that occurs under similar wind and humidity conditions from a saturated surface at the actual temperature (Granger and Gray, 1989).

# HESSD

10, 13595–13634, 2013

## A universal evapotranspiration model

F. M. Anayah and  
J. J. Kaluarachchi

Title Page

Abstract

Introduction

Conclusions

References

Tables

Figures

⏪

⏩

◀

▶

Back

Close

Full Screen / Esc

Printer-friendly Version

Interactive Discussion



## A universal evapotranspiration model

F. M. Anayah and  
J. J. Kaluarachchi

Title Page

Abstract

Introduction

Conclusions

References

Tables

Figures

⏪

⏩

◀

▶

Back

Close

Full Screen / Esc

Printer-friendly Version

Interactive Discussion

In such a case the procedure described by Allen et al. (2005, Eq. E.5) is followed. One major difference between the CRAE and ASCE methods is the albedo calculation. In the former, albedo is calculated using a set of equations whereas albedo is fixed at 0.23 in the latter. The ASCE method also requires wind speed measurements to calculate ETP while estimating crop ET requires detailed information of land cover/land use, crops, cropping pattern and the growing cycle. The ASCE method is specifically utilized in this study to compare  $R_{ASCE}$  with  $R_T$  and  $R_{TP}$ . The ASCE method is also used to calculate  $G_{soil}$  using the monthly averages of temperature data.

### 3 Measured flux and meteorological data

#### 3.1 Sites of EC data

In this study 34 global sites were selected with measured meteorological and flux data and these sites are distributed as follows: 17 from AmeriFlux sites, 11 from EuroFlux sites, five from AsiaFlux sites and one CarboAfrica site (see Fig. 2). Unfortunately, efforts to obtain data from other sites in CarboAfrica have not been successful. The selection of the 34 sites was based on data availability and climatic variability. The details of the sites and data collected are shown in Table 1 and Fig. 2.

The reason to select 34 sites is that prior studies have typically used less number of sites and in most cases under similar climatic conditions. By using a variety of global sites in contrasting physical and climatic conditions with measured ET data, we will demonstrate the validity of the proposed complementary method in different land use/land class categories. While there are other EC global sites, these sites could not be considered due to the lack of diversity of land classes and climatic conditions required in this study. As mentioned earlier, data accessibility was also an issue in some cases.

To classify the climatic conditions prevailing at each site, a simple aridity index developed by De Martonne (1925),  $AI_M$  (in  $\text{mm}^\circ\text{C}^{-1}$ ), is chosen and given as

$$AI_M = \frac{P_{\text{ann}}}{T_{\text{ann}} + 10} \quad (14)$$

where  $P_{\text{ann}}$  is the average annual precipitation in mm and  $T_{\text{ann}}$  is the average annual  $T$  in  $^\circ\text{C}$ . Unlike other aridity indices,  $AI_M$  indicates the availability of both water and energy from readily available data. In effect, the sites were sorted to the following climatic classes; very humid ( $AI_M \geq 35$ ), humid ( $28 \leq AI_M < 35$ ), sub-humid ( $24 \leq AI_M < 28$ ), Mediterranean ( $20 \leq AI_M < 24$ ), semi-arid ( $10 \leq AI_M < 20$ ) and arid ( $AI_M < 10$ ).

As shown in Table 1, the 34 sites have different geographic and climatic conditions. The dataset consists of 1657 monthly measurements across the 34 sites. The  $P_{\text{ann}}$  values range from 196 mm at site 25 to 2231 mm at site 4, and  $T_{\text{ann}}$  varies between  $-1.7^\circ\text{C}$  at site 3 and  $26.3^\circ\text{C}$  at site 4. It is noticed that many sites fall within the very humid climatic class. The surface conditions also differ considerably from grasslands to forests. Data are available from 12 to 120 months from 1992 to 2010. At site 1, for example, data from 24 months are available in 2006 and 2007, while at site 4 there are no ET data in April 2003. Therefore, the total number of months included in the calculations from 2002 to 2005 is 47 instead of 48. Compared to the lowest average  $ET_{\text{EC}}$  flux ( $10.5 \text{ mm month}^{-1}$ ) that occurs at site 25, site 4 has the maximum of  $134.3 \text{ mm month}^{-1}$ . It is observed that site 4 has the highest  $ET_{\text{EC}}$  fluxes across the 34 sites because the site is located in tropical peat swamp forests where soil moisture is relatively high throughout the year (Hirano et al., 2005) and the site is also exposed to high energy demands. In general, the wide ranges of  $ET_{\text{EC}}$  fluxes and  $AI_M$  values reflect the diversity of hydrologic and climatic conditions present in this study.

### 3.2 Measured flux data from EC systems

In comparison to finer resolution data, collecting data at monthly scale is easier in rural and sparse areas, less problematic when data quality is poor and more appropriate for

## A universal evapotranspiration model

F. M. Anayah and  
J. J. Kaluarachchi

Title Page

Abstract

Introduction

Conclusions

References

Tables

Figures

⏪

⏩

◀

▶

Back

Close

Full Screen / Esc

Printer-friendly Version

Interactive Discussion



## A universal evapotranspiration model

F. M. Anayah and  
J. J. Kaluarachchi

Title Page

Abstract

Introduction

Conclusions

References

Tables

Figures

⏪

⏩

◀

▶

Back

Close

Full Screen / Esc

Printer-friendly Version

Interactive Discussion

regional-scale studies. Thompson et al. (2011) examined model performance using different time scales from half hourly to inter-annual and found that a monthly time step is preferable. Data in this study were directly downloaded from its regional network website and sometimes obtained (or complemented) through personal communications. In cases where monthly data were not readily available, average monthly data were aggregated from finer time resolution data, e.g., daily or hourly. To keep minimal changes to the input data, months of available data (50 % or more) only were considered in the analysis.

Input data requirements are often the driver to select a specific method to estimate ET. Even in rural regions where data limitations are common, data to calculate  $R_n$  from the CRAE method (Morton, 1983) include monthly averages of temperature, humidity (or dew-point temperature) and sunshine hours (or solar radiation) only. Again, the CRAE method calculates two types of  $R_n$ ;  $R_T$  and  $R_{TP}$  at the same time. It is obvious that the CRAE method can also estimate ETP, ETW and ET using the same data. However, both AA and GG methods, similar to any classical method, need wind speed measurements to calculate ET (see Eq. 6). The performance indicators used to assess the model predictions are root mean square error (RMSE), mean absolute bias (BIAS) and coefficient of determination ( $R^2$ ). As the number of sites is large, the absolute value of mean bias (BIAS), which indicates the disparity of predicted and measured ET, is preferred over the mean bias value itself because negative values of mean bias cannot cancel positive values.

## 4 Model development and results

The approach used here is a systematic model sensitivity analysis across the three existing complementary methods to identify the major model components contributing to predicting ET compared to the EC observations. The findings from each step of the sensitivity analysis is later used to propose a universal model that is calibration-free and capable of predicting ET (or total water loss) independent of land cover/use. The



estimates are not close enough to the  $ET_{EC}$  measurements indicating that there is a need for improvements to the existing methods.

## 4.2 Development of alternative model variations

The prior estimates of ET are highly dependent on  $R_n$ . Net radiation computed by Morton (1983) is denoted as  $R_T$  which is net radiation at  $T$  while  $R_{TP}$  is net radiation at  $T_P$ . Net radiation from Allen et al. (2005) is denoted as  $R_{ASCE}$ . When compared to the  $R_n$  measurements from the EC sites, the three estimates of net radiation perform better as humidity increases. Although detailed results are not shown here, the average  $R^2$  values of  $R_T$  and  $R_{ASCE}$  estimates range from 88 to 98% and from 92 to 98%, respectively. While  $R_{ASCE}$  is the overall best estimator of  $R_n$ ,  $R_T$  performs better in arid and semi-arid regions. The results of this analysis clearly indicate that the net radiation prediction is dependent on the climatic class and therefore, any improvements should consider climate dependency. Selecting the correct equations to calculate ETP, ETW and even ET may be significantly influenced by the accuracy of the net radiation estimates.

In Stage 2, different combinations of model formulations are considered to develop a set of alternative model variations that may be better than the original methods. For instance, these alternative model variations can decide if  $R_T$  is a better estimator of the net radiation compared to  $R_{ASCE}$  or not. Similarly another question is if the complementary relationships are adequately presented by Eq. (1) or Eq. (8) or a different formulation is needed. In selecting these different alternative model variations, the criteria for the sensitivity analysis used are; the method to calculate  $R_n$ , the representation of the complementary relationship, the value of  $\alpha$  in the  $ET_{PT}$  equation, the value of  $\beta$  in the wind function of the  $ET_{PEN}$  equation and the relative evaporation function ( $G$ ) of the GG method. After studying the model structure of each complementary method, 17 different alternative model variations are proposed in Table 3 for subsequent analysis. As discussed earlier, this is a systematic parameter sensitivity exercise to identify the best alternative model variation. Although more model variations are possible, the

### A universal evapotranspiration model

F. M. Anayah and  
J. J. Kaluarachchi

Title Page

Abstract

Introduction

Conclusions

References

Tables

Figures

⏪

⏩

◀

▶

Back

Close

Full Screen / Esc

Printer-friendly Version

Interactive Discussion



# HESSD

10, 13595–13634, 2013

## A universal evapotranspiration model

F. M. Anayah and  
J. J. Kaluarachchi

Title Page

Abstract

Introduction

Conclusions

References

Tables

Figures

⏪

⏩

◀

▶

Back

Close

Full Screen / Esc

Printer-friendly Version

Interactive Discussion

17 listed alternative model variations are adequate at this stage. For example, the AA and GG methods have four criteria each ( $R_n$ , complementary relationship,  $\alpha$  and  $\beta$ ) producing 16 model variations. An important consideration in the development of these model variations is the conclusions of others. For instance, Hobbins et al. (2001) found that changes to the AA method did not necessarily produce superior results especially by perturbing  $\beta$  (see Brutsaert and Stricker, 1979).

The ET estimates produced by these 17 alternative model variations across the 34 sites were compared to the EC measurements and the results are shown in Fig. 3. It should be noted that Fig. 3 shows the anomalies from the original method for each model variation. In effect, the results are considered to show improvements if the anomaly of RMSE is negative. The same trend is valid for BIAS but opposite for  $R^2$ . It is observed that none of the CRAE- or AA-based alternative model variations improved RMSE and BIAS. Among the CRAE-based model variations, CRAE2 has the minimum deterioration of RMSE and BIAS while showing some improvement of  $R^2$ . A similar behavior is noticed with AA4 of the AA-based model variations. However, the GG-based model variations have obvious improvements across all three metrics. GG1, GG3, GG5 and GG7 model variations showed improved RMSE and BIAS values when compared with the original GG method. The only common feature among these four GG model variations is Eq. (1) representing the complementary relationship and not Eq. (8) which was used by the original GG method. This observation indicates that Eq. (1) is superior in representing the complementary relationship between ET, ETW and ETP. The deterioration of results in the GG-based model variations is deemed minor when compared to the other model variations. The conclusion from Stage 2 is that these GG model variations perform better than the CRAE and AA model variations.

One important difference of the original GG method compared to the other two methods is the equation describing ETW. ETW of the original CRAE and AA methods is derived from the  $ET_{PT}$  equation (Eq. 7) while the original GG method uses the  $ET_{PEN}$  equation or Eq. (5) (Brutsaert and Stricker, 1979; Granger and Gray, 1989; Morton, 1983). Given this departure of the GG model from others, we further studied the GG

model variations based on the model describing ETW. Accordingly, another set of alternative model variations from the GG model is possible. These variations consist of 16 models (GG8 through GG23) and the details are given in Table 4. In these variations,  $\beta$  is no longer changed while  $\alpha$  in the  $ET_{PT}$  equation will be changed. ETW in all these variations will use the Priestley–Taylor equation (see Table 4). In total, 23 GG model variations (GG1 through GG23 from Tables 3 and 4) are now considered for the next stage.

### 4.3 Selection of best performing GG model variation(s)

For the purpose of selecting the best GG model variation(s), each model from the latest 23 was run and the results were compared with EC observations (see Table 5). The performance metrics were used to identify the best GG model variation in each climatic and performance metric combination and the results are shown in Table 5. For example, GG3 was the best for RMSE, GG1 for BIAS and GG17 and GG23 for  $R^2$  in the very humid class. In essence, 11 GG model variations became eligible from the 23 selected earlier from Stage 2. It is also observed that GG20 is the best for six combinations of performance metric and climatic class. In contrast, GG3 is the best only in RMSE for the very humid class. GG1, GG3, GG11 and GG13 are the best models each for one combination of performance metric and climatic class only. Therefore these GG model variations were rejected and the remaining seven (GG7, GG14, GG17, GG18, GG20, GG22 and GG23) were selected for further consideration.

There are other key observations made from the prior analysis. First, the original GG method uses the complementary relationship given by Eq. (8) (Granger, 1989), yet, five of the seven promising model variations selected earlier uses Eq. (1). In essence, this observation suggests that Eq. (1) is better in capturing the variability of ET compared to Eq. (8). Second, six of these seven promising GG model variations use  $ET_{PT}$  equation to calculate ETW. Third, a comparison between  $R_T$  and  $R_{ASCE}$  shows that six of these promising GG model variations use  $R_{ASCE}$  to denote the net radiation and this supports the conclusion drawn earlier. Fourth, five of these GG model variations use Eq. (12)

## A universal evapotranspiration model

F. M. Anayah and  
J. J. Kaluarachchi

Title Page

Abstract

Introduction

Conclusions

References

Tables

Figures

⏪

⏩

◀

▶

Back

Close

Full Screen / Esc

Printer-friendly Version

Interactive Discussion



to calculate  $G$ . Lastly, changing the value of  $\alpha$  in the  $ET_{PT}$  equation and varying the equation describing  $G$  did not alter the results.

The next step of the analysis will be to identify the best model variation of the seven selected earlier. Before proceeding to the next step, the six climatic classes are simplified to represent climatic variability using three simple classes; wet (from original very humid and humid), moderate (from original sub-humid and Mediterranean) and dry (from original semi-arid and arid). This revision shall not affect the results and will make the analyses and conclusions simple. Using these new definitions, the original 34 global sites are now reallocated as 18, 6 and 10 into wet, moderate and arid classes, respectively.

Figure 4 shows the results of performance metrics to these seven models using the simplified climatic classes of wet, moderate and dry. For all climatic classes, GG17 has the highest RMSE and GG7 has the highest BIAS values. GG7 performs well only in the wet climatic class, while it performs poor in the moderate and dry classes. The GG17 and GG23 model variations have identical behaviors since these differ in the  $\alpha$  value only. Both models fail in the moderate climatic class. It is also noticed that GG14 does not simulate ET well in the moderate climatic class.

Overall, GG22 has the lowest median and average values of RMSE that are 16.20 and 20.23  $\text{mm month}^{-1}$ , respectively. These results indicate that GG22 has the potential to be the best model variation. Based on BIAS for all sites, the lowest average value is 10.55  $\text{mm month}^{-1}$  for GG18, while the lowest median value is 7.45  $\text{mm month}^{-1}$  for GG20. Comparing the three model variations, both GG18 and GG20 have same  $R^2$  of 0.64 and GG22 produced 0.62. It is therefore reasonable to state that GG18, GG20 and GG22 are the best GG model variations for further consideration.

There is no evidence to suggest that a specific model variation from these three models is superior in a particular climatic class. The climatic class with poorest performance is the moderate class. The reason may be the low number of sites in this class and therefore extreme values such as those of site 24 can dramatically influence the results. In the moderate climatic class, GG22 has the lowest average RMSE and

**A universal evapotranspiration model**

F. M. Anayah and  
J. J. Kaluarachchi

Title Page

Abstract

Introduction

Conclusions

References

Tables

Figures

⏪

⏩

◀

▶

Back

Close

Full Screen / Esc

Printer-friendly Version

Interactive Discussion



BIAS, however, GG18 and GG20 share the highest average  $R^2$ . It is also noted that all three model variations have the following similarities; the net radiation is calculated by  $R_{ASCE}$ , the complementary relationship is represented by Eq. (1) and the ETW is computed by Eq. (7).

#### 4.4 Statistical analysis

The applicability of the three GG model variations, GG18, GG20 and GG22, is further investigated using the analysis of variance (ANOVA) test to assess if these three models are similar or not (see Berthouex and Brown, 2002). The ANOVA test was used on the time-series consisting of 1657 estimates of ET from each model variation and measured  $ET_{EC}$ . The average values of ET across the 34 sites are 35.9, 33.8, 33.2 and 32.0 mm month<sup>-1</sup>, for measured data, GG18, GG20 and GG22, respectively. There is a tendency to underestimate average ET by all three model variations. The reason may be the similarity in structure of the three GG model variations. The ANOVA  $F$  test statistic ( $F_{V1, V2, 1-CI}$ ) was computed for the four time-series (simulated 3 GG model variations and  $ET_{EC}$  observations) at 95 % confidence level (V1 is the number of models minus 1, V2 is the number of measurements minus the number of models and CI is the confidence interval) and compared to that of the  $F$  test of ANOVA. Simply, if the  $F$  test is smaller, methods are alike. In this case,  $F_{3, 1653, 0.05}$  is found to be 2.60 (Berthouex and Brown, 2002, Table C in Appendix) while the  $F$  test is 4.58. Therefore, it is obvious at 95 % confidence, the averages of the four time series are not equal; however, the test cannot identify which model variation is different than the others.

For this purpose, Dunnet's method (Berthouex and Brown, 2002) was used to compare the three GG model variations to the measured  $ET_{EC}$  fluxes. The Dunnet's method has the advantage to answer two questions; a confidence interval in which average values are alike and the direction of the difference. The results of the Dunnet's method showed that at 95 % confidence interval, the average ET is between 32.3 and 39.4 mm month<sup>-1</sup>. In other words, GG22 is statistically different while the difference in

## A universal evapotranspiration model

F. M. Anayah and  
J. J. Kaluarachchi

Title Page

Abstract

Introduction

Conclusions

References

Tables

Figures

⏪

⏩

◀

▶

Back

Close

Full Screen / Esc

Printer-friendly Version

Interactive Discussion



# HESSD

10, 13595–13634, 2013

## A universal evapotranspiration model

F. M. Anayah and  
J. J. Kaluarachchi[Title Page](#)[Abstract](#)[Introduction](#)[Conclusions](#)[References](#)[Tables](#)[Figures](#)[⏪](#)[⏩](#)[◀](#)[▶](#)[Back](#)[Close](#)[Full Screen / Esc](#)[Printer-friendly Version](#)[Interactive Discussion](#)

each of the other two model variations is likely to be insignificant. Figure 5 shows the average ET estimates across 33 sites according to the climatic class. At site 4, none of the models can simulate the elevated ET fluxes measured. In general, GG22 underestimates ET as humidity increases. However, the scatter of data around the 1 : 1 line for most climatic classes is more pronounced with GG18 and GG20. The similarity between GG18 and GG20 is visible because the only difference between the two models is  $\alpha$  in the  $ET_{PT}$  equation that does not influence the results. In fact, GG18 has two advantages over the other two model variations; it has the closest average ET value to that of the  $ET_{EC}$  fluxes and is the closest to the 1 : 1 line (see Fig. 5). Hence, GG18 is deemed to be the best from the seven promising GG model variations.

In Fig. 6, the performance metrics of GG18 are shown for each site in the three climatic classes. The  $R^2$  values have a minor increasing trend with humidity. The  $R^2$  values at sites of wet climatic class mostly lie above the average value and vice versa for the dry climatic class. There is no such a trend with RMSE and BIAS. However, the RMSE and BIAS values at most sites of the dry climatic class are below the average value. Again, it is emphasized that site 4 has specific data issues that have to be further inspected. Generally, Fig. 6 demonstrates that GG18 is consistently predicting ET across these 34 sites that have diverse climatic and physical conditions.

The average  $R^2$  values of GG18 over the wet, moderate and dry classes are 0.72, 0.61 and 0.52, respectively. Since the ET fluxes differ between the wet and dry climates, the absolute values of RMSE may not be simply compared to each other. Instead, the RMSE value at each site is divided by the average  $ET_{EC}$  value shown in Table 1 such that the relative RMSE is computed and compared across all sites. The values of relative RMSE for GG18 range from 0.23 at site 11 to 1.59 at site 34 with an average of 0.69.

## 4.5 Comparison with recent studies

In this section, the results of the proposed modified complementary method, specifically GG18, are compared to the results from recently published studies using the classical and complementary methods.

5 Suleiman and Crago (2004) estimated hourly ET using radiometric surface temperatures in two grassland sites in Oklahoma and Kansas and validated results using EC data. The results showed the RMSE values ranged from 32 to 53 mm month<sup>-1</sup> while  $R^2$  varied between 0.78 and 0.94. Mu et al. (2007) used data from 19 AmeriFlux EC sites to validate the estimates of a remotely sensed ET using a revised Penman–Monteith equation. The average RMSE, bias and  $R^2$  were 29 mm month<sup>-1</sup>, -6 mm month<sup>-1</sup> and 0.76, respectively. When used with 46 AmeriFlux sites (Mu et al., 2011), the results showed average RMSE, absolute bias and  $R^2$  of 26 mm month<sup>-1</sup>, 10 mm month<sup>-1</sup> and 0.65, respectively. Kuske (2009) estimated ET using Penman–Monteith and Priestley–Taylor equations and compared estimates to EC data. Both models were significantly overestimating high ET fluxes and slightly underestimating low ET fluxes. Thompson et al. (2011) tested an ET “null” model that coupled the Penman–Monteith equation to a soil moisture model at 14 AmeriFlux sites from which eight sites are used in the present study. RMSE varied between 56 and 208 mm month<sup>-1</sup> and therefore, changes were made to further improve the model to produce RMSEs of 34 to 175 mm month<sup>-1</sup>.

20 However, complementary methods to predict ET have not been extensively compared with EC-based ET measurements. With the exception of Ali and Mawdsley (1987), researchers have recently started paying attention to the complementary methods. A monthly ET map using a modified Morton method was produced using MODIS imagery for Hungary (Szilagyi and Kovacs, 2010) and verified using three EC sites. At two sites,  $R^2$  values were 0.79 and 0.80 and bias ranged between -19 and 21 mm month<sup>-1</sup>. At the third site, however, the authors found a difference of 44 % with the EC measurements. Shifa (2011) examined the wind function of the AA method using data under wet and dry conditions. With the original AA method, RMSE was 17 and

HESSD

10, 13595–13634, 2013

### A universal evapotranspiration model

F. M. Anayah and  
J. J. Kaluarachchi

Title Page

Abstract

Introduction

Conclusions

References

Tables

Figures

⏪

⏩

◀

▶

Back

Close

Full Screen / Esc

Printer-friendly Version

Interactive Discussion

## A universal evapotranspiration model

F. M. Anayah and  
J. J. Kaluarachchi

Title Page

Abstract

Introduction

Conclusions

References

Tables

Figures

⏪

⏩

◀

▶

Back

Close

Full Screen / Esc

Printer-friendly Version

Interactive Discussion

29 mm month<sup>-1</sup> for the wet and dry conditions, respectively. The author found that the AA method performed best using calibrated wind function coefficients under wet conditions in which RMSE and  $R^2$  were 12 mm month<sup>-1</sup> and 0.7, respectively. Huntington et al. (2011) tested the AA method using data from arid shrublands at five EC sites in eastern Nevada. It was found that RMSE,  $R^2$  and percent bias were 13 mm month<sup>-1</sup>, 0.77 and 18 %, respectively. RMSE,  $R^2$  and percent bias of a modified AA method were 11 mm month<sup>-1</sup>, 0.71 and 1 %, respectively. Han et al. (2011) proposed an enhanced GG model at four sites under different land covers and compared results to the original GG method and EC-based ET data. The enhanced model was better than the original GG method at three sites and RMSE of the enhanced GG model ranged from 4 to 16 mm month<sup>-1</sup>.

Table 6 shows the results from a set of the abovementioned studies compared with the results of the proposed GG18 model variation. The comparison shows that the results of the GG18 model variation are equal or better and more reliable considering the wide range of physical and climatic conditions of the 34 global EC sites used in this study. More importantly, the ET estimates of GG18 outperform the estimates of ET of other studies given the minimal cost and data needed to compute reliable regional ET using meteorological data only. Furthermore, GG18 is a single-step method that does not require local calibration and therefore suitable to use in rural river basins with minimal data and monitoring while providing the total water loss from the land surface that is appropriate in water resources planning. The model structure of the proposed GG18 model variation is given in Fig. 7.

## 5 Summary and conclusions

Complementary methods have the potential to predict regional ET using minimal meteorological data. However, prior studies used small data sets representing limited climatic variability and physical conditions that were not successful in improving the methods. A few of the successful studies used locally calibrated parameters that may not

## A universal evapotranspiration model

F. M. Anayah and  
J. J. Kaluarachchi

Title Page

Abstract

Introduction

Conclusions

References

Tables

Figures

⏪

⏩

◀

▶

Back

Close

Full Screen / Esc

Printer-friendly Version

Interactive Discussion

have the universal applicability simply due to the two-step approach required to compute ET. In addition, water resources studies require the total water loss from the land surface irrespective of the land use/land class. In this regard, complementary methods provide the distinct advantage over the classical methods that only provide crop ET using detailed input data such as land use/land class, cropping patterns and crop calendar. The state of the complementary methods is such that there is no single methodology consistently used over a wide variety of climatic and physical conditions. This study is aimed at developing calibration-free universal model using the complementary relationship that requires meteorological data only to predict regional ET.

In this work, 34 global sites with measured ET data via the EC method are used to develop the proposed model using systematic sensitivity analysis conducted with the three original complementary methods. The sites have different climatic and physical conditions to ensure the universal application of the proposed model. The three original complementary methods consisting of CRAE, AA and GG are first evaluated and the need for improvement to all methods is determined. Based on the model structures, 20 alternative model variations are proposed. The GG method is found to be the most attractive compared to the other two methods and therefore the GG method is further analyzed. ETW that uses Priestley–Taylor equation produced 16 GG model variations. Climates of the FLUXNET sites were initially sorted to six climatic classes based on the aridity index proposed by De Martonne (1925). The initial results identified seven promising model variations out of the 23 GG-based ones. Given the complexity of using six different climatic classes, the analysis later reduced this number to three distinct climatic classes consisting of wet, moderate and dry climates. This simplification identified three promising model variations from the earlier seven variations. Statistical analyses conducted via ANOVA testing and the Dunnet method showed that two of the model variations are similar while one GG model variation, GG18, clearly provided a different distribution and results. Therefore the GG18 model variation is considered the best. Also the comparison of results from recent studies shows that the GG18

model variation is capable of producing equal or better results while capturing a wide variety of physical and climatic conditions.

In the proposed GG18 model, the net radiation  $R_n$  is computed using  $R_{ASCE}$  calculated by Allen et al. (2005) which outperforms  $R_T$  developed by Morton (1983). It is evident that the simple complementary relationship suggested by Eq. (1) can describe the behavior of ET fluxes better than the more generic complementary relationship of Eq. (8). Most importantly, the predictive power of the GG method (Granger and Gray, 1989) is improved when the  $ET_{PT}$  equation is used to calculate ETW. There is a strong indication that the proposed GG18 model can significantly enhance the accuracy of ETW using the GG method and consequently to predict regional ET using meteorological data only and without calibration. Furthermore, this one-step estimation method can reliably estimate ET regardless of the prevailing climatic conditions. Such an estimate will unequivocally lead to reliable predictions of water resources, in particular recharge estimation and impacts due to climate change.

*Acknowledgements.* This study was supported by the Utah Water Research Laboratory of Utah State University with additional funding available from the International Water Management Institute, Sri Lanka. We thank Vladimir Smakhtin and Paul Pavelic for their support and encouragement. The authors would like to acknowledge all scientists of FLUXNET agencies and Naama Raz-Yaseef from University of California, Berkeley for their willingness to share data. The assistance of David Stevens, Luis Bastidas and David Tarboton from Utah State University is appreciated. The English of the manuscript had been kindly edited by Naomi Higham.

## References

- Ali, M. F. and Mawdsley, J. A.: Comparison of two recent models for estimating actual ET using only regularly recorded data, *J. Hydrol.*, 93, 257–276, doi:doi:10.1016/0022-1694(87)90099-0, 1987.
- Allen, R. G., Pereira, L. S., Raes, D., and Smith, M. (Eds.): *Crop Evapotranspiration: Guidelines for Computing Crop Water Requirements*, FAO Irrig. Drain., Paper No. 56, Food and Agr. Orgn. of the United Nations, Rome, Italy, 1998.

## A universal evapotranspiration model

F. M. Anayah and  
J. J. Kaluarachchi

Title Page

Abstract

Introduction

Conclusions

References

Tables

Figures

⏪

⏩

◀

▶

Back

Close

Full Screen / Esc

Printer-friendly Version

Interactive Discussion



## A universal evapotranspiration model

F. M. Anayah and  
J. J. Kaluarachchi

Title Page

Abstract

Introduction

Conclusions

References

Tables

Figures

⏪

⏩

◀

▶

Back

Close

Full Screen / Esc

Printer-friendly Version

Interactive Discussion

- Allen, R. G., Walter, I. A., Elliot, R., Howell, T., Itenfisu, D., and Jensen, M. (Eds.): The ASCE Standardized Reference Evapotranspiration Equation, Environment and Water Resources Institute of the Am. Soc. Civil Eng. (ASCE), Task Committee on Standardization of Reference Evapotranspiration, Final Rep., ASCE, Reston, VA, USA, 2005.
- 5 Baldocchi, D., Falge, E., Gu, L., Olson, R., Hollinger, D., Running, S., Anthoni, P., Bernhofer, C., Davis, K., Evans, R., Fuentes, J., Goldstein, A., Katul, G., Law, B., Lee, X., Malhi, Y., Meyers, T., Munger, W., Oechel, W., Paw, K. T., Pilegaard, K., Schmid, H. P., Valentini, R., Verma, S., Vesala, T., Wilson, K., and Wofsy, S.: FLUXNET: a new tool to study the temporal and spatial variability of ecosystem-scale carbon dioxide, water vapor, and energy flux densities, *B. Am. Meteorol. Soc.*, 82, 2415–2434, doi:10.1175/1520-0477(2001)082<2415:FANTTS>2.3.CO;2, 2001.
- 10 Berthouex, P. and Brown, L. (Eds.): *Statistics for Environmental Engineers*, 2nd Edn., Lewis publishers, CRC Press LLC, Boca Raton, FL, 2002.
- Bouchet, R. J.: Evapotranspiration réelle et potentielle, signification climatique, in: *General Assembly Berkeley*, Publ. No. 62, Int. Assoc. Sci. Hydrol., Gentbrugge, Belgium, 134–142, 1963.
- 15 Brutsaert, W. and Stricker, H.: An advection aridity approach to estimate actual regional evaporation, *Water Resour. Res.*, 15, 443–450, doi:10.1029/WR015i002p00443, 1979.
- Castellvi, F. and Snyder, R. L.: A comparison between latent heat fluxes over grass using a weighing lysimeter and surface renewal analysis, *J. Hydrol.*, 381, 213–220, doi:10.1016/j.jhydrol.2009.11.043, 2010.
- 20 Castellvi, F., Snyder, R. L., and Baldocchi, D. D.: Surface energy-balance closure over rangeland grass using the eddy covariance method and surface renewal analysis, *Agr. Forest Meteorol.*, 148, 1147–1160, doi:10.1016/j.agrformet.2008.02.012, 2008.
- 25 Davenport, D. C. and Hudson, J. P.: Changes in evaporation rates along a 17-km transect in the Sudan Gezira, *Agr. Meteorol.*, 4, 339–352, 1967.
- De Martonne, E. (Eds.): *Traité de Géographie Physique*, tome 1, 4th Edn., A. Colin, Paris, 1925.
- Doyle, P.: Modelling catchment evaporation: an objective comparison of the Penman and Morton approaches, *J. Hydrol.*, 121, 257–276, 1990.
- 30 FAO (Eds.): *Arid zone forestry: a guide for field technicians*, in: *FAO Conservation Guide 20*, Food and Agr. Org. of the United Nations, Rome, Italy, 1989.



## A universal evapotranspiration model

F. M. Anayah and  
J. J. Kaluarachchi

Title Page

Abstract

Introduction

Conclusions

References

Tables

Figures

⏪

⏩

◀

▶

Back

Close

Full Screen / Esc

Printer-friendly Version

Interactive Discussion

matic synthesis, *Hydrol. Earth Syst. Sci.*, 17, 1331–1363, doi:10.5194/hess-17-1331-2013, 2013.

Morton, F. I.: Operational estimates of areal evapotranspiration and their significance to the science and practice of hydrology, *J. Hydrol.*, 66, 1–76, doi:10.1016/0022-1694(83)90177-4, 1983.

Mu, Q., Heinsch, F. A., Zhao, M., and Running, S. W.: Development of a global evapotranspiration algorithm based on MODIS and global meteorological data, *Remote Sens. Environ.*, 111, 519–536, doi:10.1016/j.rse.2007.04.015, 2007.

Mu, Q., Zhao, M., and Running, S. W.: Improvements to a MODIS global terrestrial evapotranspiration algorithm, *Remote Sens. Environ.*, 115, 1781–1800, doi:10.1016/j.rse.2011.02.019, 2011.

Penman, H. L.: Natural evaporation from open water, bare soil, and grass, *Roy. Soc. Lond. A*, 193, 120–145, doi:10.1098/rspa.1948.0037, 1948.

Penman, H. L.: Evaporation: an introductory survey, *Neth. J. Agr. Sci.*, 4, 9–29, 1956.

Pettijohn, J. C. and Salvucci, G. D.: A new two-dimensional physical basis for the complementary relation between terrestrial and pan evaporation, *J. Hydrometeorol.*, 10, 565–574, doi:10.1175/2008JHM1026.1, 2009.

Priestley, C. H. B. and Taylor, R. J.: On the assessment of surface heat flux and evaporation using large-scale parameters, *Mon. Weather Rev.*, 100, 81–92, doi:10.1175/1520-0493(1972)100<0081:OTAOSH>2.3.CO;2, 1972.

Shifa, Y. B.: Estimation of evapotranspiration using advection aridity approach, M.Sc. thesis, University of Twente, the Netherlands, 52 pp., 2011.

Suleiman, A. and Crago, R.: Hourly and daytime ET from grassland using radiometric surface temperatures, *Agron. J.*, 96, 384–390, 2004.

Szilagyi, J. and Kovacs, A.: Complementary-relationship-based evapotranspiration mapping (cremap) technique for Hungary, *Periodica Polytech.*, 54, 95–100, doi:10.3311/pp.ci.2010-2.04, 2010.

Szilagyi, J. and Kovacs, A.: A calibration-free evapotranspiration mapping technique for spatially-distributed regional-scale hydrologic modeling, *J. Hydrol. Hydromech.*, 59, 118–130, doi:10.2478/v10098-011-0010-z, 2011.

Thompson, S. E., Harman, C. J., Konings, A. G., Sivapalan, M., Neal, A., and Troch, P. A.: Comparative hydrology across AmeriFlux sites: the variable roles of climate, vegetation, and groundwater, *Water Resour. Res.*, 47, W00J07, doi:10.1029/2010WR009797, 2011.

# HESSD

10, 13595–13634, 2013

## A universal evapotranspiration model

F. M. Anayah and  
J. J. Kaluarachchi[Title Page](#)[Abstract](#)[Introduction](#)[Conclusions](#)[References](#)[Tables](#)[Figures](#)[⏪](#)[⏩](#)[◀](#)[▶](#)[Back](#)[Close](#)[Full Screen / Esc](#)[Printer-friendly Version](#)[Interactive Discussion](#)

Twine, T., Kustas, W. P., Norman, J. M., Cook, D. R., Houser, P. R., Meyers, T. P., Prueger, J. H., Starks, P. J., and Wesely, M. L.: Correcting eddy-covariance flux underestimates over a grassland, *Agr. Forest Meteorol.*, 103, 279–300, doi:10.1016/S0168-1923(00)00123-4, 2000.

5 Wang, T., Sammis, W., and Miller, D. R.: Eddy covariance measurements of crop water uses: the energy closure problem and potential solutions, in: *Agricultural Water Management Research Trends*, Nova Science Publishers Inc., New York, USA, 1–7, 2008.

10 Wilson, K., Goldstein, A., Falge, E., Aubinet, M., Baldocchi, D., Berbigier, P., Bernhofer, C., Ceulemans, R., Dolman, H., Field, C., Grelle, A., Ibrom, A., Law, B. E., Kowalski, A., Meyers, T., Moncrieff, J., Monson, R., Oechel, W., Tenhunen, J., Valentini, R., and Verma, S.: Energy balance closure at FLUXNET sites, *Agr. Forest Meteorol.*, 113, 223–243, doi:10.1016/S0168-1923(02)00109-0, 2002.

15 Xu, C. Y. and Singh, V. P.: Evaluation of three complementary relationship evapotranspiration models by water balance approach to estimate actual regional evapotranspiration in different climatic regions, *J. Hydrol.*, 308, 105–121, doi:10.1016/j.jhydrol.2004.10.024, 2005.

## A universal evapotranspiration model

F. M. Anayah and  
J. J. Kaluarachchi

**Table 1.** Characteristics of the 34 EC sites with measured ET data used in the study.

#	Site	Country	Lat. °	Long. °	Data availability from-to (# months)	ET <sub>EC</sub> , mm month <sup>-1</sup>			Al <sub>M</sub> , mm °C <sup>-1</sup>	Land cover
						min	mean	max		
Very humid										
1	Takayama	Japan	36.1	137.4	06–07 (24)	9.4	44.4	91.7	83.2	Coniferous forest
2	Walker Branch, TN	USA	36.0	-84.3	95–98 (48)	10.5	47.4	116.2	76.5	Deciduous forest
3	Qinghai	China	37.6	101.3	02–04 (36)	1.6	36.2	110.5	68.3	Alpine meadow
4	Palangkaraya	Indonesia	2.3	114.0	02–05 (47)	82.4	134.3	164.0	61.5	Tropical forest
5	Harvard Forest, MA	USA	42.5	-72.2	92–99 (96)	5.1	37.5	108.4	61.2	Mixed forest
6	Flakaliden	Sweden	64.2	19.8	96–98 (31)	-0.1	23.0	63.4	51.5	Coniferous forest
7	Bondville, IL	USA	40.0	-88.3	97–06 (120)	1.7	50.1	135.4	49.6	Cropland
8	Goodwin Creek, MS	USA	34.3	-89.9	03–06 (48)	2.4	55.5	138.7	47.9	Cropland
9	Tharandt	Germany	51.0	13.6	96–99 (42)	6.5	39.2	95.9	47.1	Coniferous forest
10	Sarrebouurg	France	48.7	7.1	96–99 (32)	-0.1	32.8	102.3	42.7	Deciduous forest
11	Kennedy Oak, FL	USA	28.6	-80.7	02–06 (48)	6.0	49.1	120.3	40.4	Evergreen forest
12	Loobos	Netherland	52.2	5.7	96–98 (30)	7.4	32.4	63.1	39.7	Coniferous forest
13	Sakaerat	Thailand	14.5	101.9	01–03 (32)	37.7	63.8	109.5	36.8	Tropical forest
Humid										
14	Norunda	Sweden	60.1	17.5	96–98 (29)	1.3	30.9	80.8	34.0	Mixed forest
15	Fort Peck, MT	USA	48.3	-105.1	00–06 (84)	1.3	26.0	164.0	33.0	Grassland
16	Freeman, TX	USA	29.9	-98.0	05–08 (48)	6.0	49.1	120.3	30.9	Grassland
17	Little Washita, OK	USA	35.0	-98.0	96–98 (32)	8.9	41.6	104.4	30.7	Grassland
18	Mehrstedt 2	Germany	51.3	10.7	04–06 (34)	0.0	27.0	95.3	29.6	Grassland
Sub-humid										
19	Evora	Portugal	38.5	-8.0	05–05 (12)	-0.3	13.7	34.8	26.2	Evergreenforest
20	Mauzac	France	43.4	1.3	05–07 (34)	8.3	37.2	91.4	25.5	Grassland
Mediterranean										
21	Bugac	Hungary	46.7	19.6	02–08 (72)	2.3	37.5	103.9	23.8	Grassland
22	Metolius, OR	USA	44.3	-121.6	04–08 (60)	2.3	30.3	71.0	22.8	Woody savanna
23	Tonzi Ranch, CA	USA	38.4	-121.0	01–09 (80)	1.4	29.8	95.5	21.0	Woody savanna
24	Vaira Ranch, CA	USA	38.4	-121.0	01–09 (108)	-5.1	25.1	88.0	21.0	Woody savanna
Semi-arid										
25	Kherlenbayan	Mongolia	47.2	108.7	03–10 (68)	-2.3	10.5	50.8	17.5	Grassland
26	Llano de los Juanes	Spain	36.9	-2.8	05–05 (12)	7.2	18.7	36.7	15.4	Oliveplantation
27	Audubon, AZ	USA	31.6	-110.5	02–09 (87)	2.0	24.4	92.5	13.5	Open shrubland
28	Kendall, AZ	USA	31.7	-109.9	04–09 (68)	2.2	20.2	72.4	13.2	Grassland
29	Santa Rita, AZ	USA	31.8	-110.9	04–07 (48)	4.3	26.0	91.1	10.7	Open shrubland
Arid										
30	Corral Pocket, UT	USA	38.1	-109.4	01–07 (39)	4.6	14.8	33.3	9.8	Grassland
31	Sevilleta grass, NM	USA	34.4	-106.7	07–08 (19)	4.5	22.2	69.7	9.0	Grassland
32	Sevilleta shrub, NM	USA	34.3	-106.7	07–08 (24)	3.3	23.5	74.7	9.0	Grassland
33	Demokeya	Sudan	13.3	30.5	97–98 (17)	6.1	38.1	106.3	8.9	Savanna/grassland
34	Yatir	Israel	31.3	35.1	01–09 (48)	5.7	17.8	57.3	8.6	Evergreen forest



[Title Page](#)

[Abstract](#)

[Introduction](#)

[Conclusions](#)

[References](#)

[Tables](#)

[Figures](#)

[⏪](#)

[⏩](#)

[⏴](#)

[⏵](#)

[Back](#)

[Close](#)

[Full Screen / Esc](#)

[Printer-friendly Version](#)

[Interactive Discussion](#)

## A universal evapotranspiration model

F. M. Anayah and  
J. J. Kaluarachchi

**Table 2.** Average values of RMSE, BIAS and  $R^2$  of actual ET estimates from the different complementary methods, CRAE, AA and GG, for each climatic class.

Climatic class	RMSE (mm month <sup>-1</sup> )			BIAS (mm month <sup>-1</sup> )			$R^2$		
	CRAE	AA	GG	CRAE	AA	GG	CRAE	AA	GG
Very humid	27.6	29.0	22.6	15.8	12.2	10.6	0.73	0.71	0.73
Humid	31.2	35.2	27.1	19.2	16.5	14.3	0.77	0.73	0.75
Sub-humid	46.6	54.7	45.0	31.9	28.7	26.5	0.39	0.33	0.41
Mediterranean	35.3	58.1	47.4	18.6	28.8	25.3	0.51	0.42	0.45
Semi-arid	16.6	18.9	22.1	9.6	8.4	13.3	0.56	0.61	0.41
Arid	22.4	31.9	29.5	9.4	14.4	19.5	0.53	0.54	0.42
All classes	27.8	33.8	28.4	15.7	15.5	15.5	0.64	0.61	0.59

[Title Page](#)
[Abstract](#)
[Introduction](#)
[Conclusions](#)
[References](#)
[Tables](#)
[Figures](#)
[⏪](#)
[⏩](#)
[◀](#)
[▶](#)
[Back](#)
[Close](#)
[Full Screen / Esc](#)
[Printer-friendly Version](#)
[Interactive Discussion](#)

## A universal evapotranspiration model

F. M. Anayah and  
J. J. Kaluarachchi

**Table 3.** Details of the 17 model variations developed based on the complementary relationships (CR) and the three original complementary methods.

Criteria Equation Value	$R_n$		CR		$\alpha$		$\beta$		$G$	
	$R_T$	$R_{ASCE}$	1	8	1.26	1.28	0.5	1.0	11	12
	CRAE	✓		✓						
CRAE1	✓			✓						
CRAE2		✓	✓							
CRAE3		✓		✓						
AA	✓		✓			✓		✓		
AA1	✓			✓		✓		✓		
AA2	✓			✓	✓		✓			
AA3		✓	✓			✓		✓		
AA4		✓		✓		✓		✓		
AA5		✓	✓		✓		✓			
AA6		✓		✓	✓		✓			
AA7	✓		✓		✓		✓			
GG	✓			✓				✓	✓	
GG1	✓		✓					✓	✓	
GG2	✓			✓				✓		✓
GG3	✓		✓					✓		✓
GG4		✓		✓				✓	✓	
GG5		✓	✓					✓		✓
GG6		✓		✓				✓		✓
GG7		✓	✓					✓		✓

Title Page

Abstract

Introduction

Conclusions

References

Tables

Figures

⏪

⏩

◀

▶

Back

Close

Full Screen / Esc

Printer-friendly Version

Interactive Discussion



# HESSD

10, 13595–13634, 2013

## A universal evapotranspiration model

F. M. Anayah and  
J. J. Kaluarachchi

**Table 4.** Sixteen GG-based model variations developed given that ET<sub>PT</sub> is calculated using ET<sub>PT</sub> equation.

Criteria Equation Value	$R_n$		CR		$\alpha$		G	
	$R_T$	$R_{ASCE}$	1	8	1.26	1.28	11	12
GG8	✓		✓		✓			✓
GG9	✓			✓	✓			✓
GG10	✓		✓		✓		✓	
GG11	✓			✓	✓		✓	
GG12	✓		✓			✓	✓	
GG13	✓			✓		✓	✓	
GG14	✓		✓			✓		✓
GG15	✓			✓		✓		✓
GG16		✓	✓			✓		✓
GG17		✓		✓		✓		✓
GG18		✓	✓			✓	✓	
GG19		✓		✓		✓	✓	
GG20		✓	✓		✓		✓	
GG21		✓		✓	✓		✓	
GG22		✓	✓		✓			✓
GG23		✓		✓	✓			✓

Title Page

Abstract

Introduction

Conclusions

References

Tables

Figures

◀

▶

◀

▶

Back

Close

Full Screen / Esc

Printer-friendly Version

Interactive Discussion



# HESSD

10, 13595–13634, 2013

## A universal evapotranspiration model

F. M. Anayah and  
J. J. Kaluarachchi

**Table 5.** Results of the performance of different models in a given climatic class described through the best values of RMSE, BIAS and  $R^2$ .

Metric	Climatic class						All classes
	Very humid	Humid	Sub-humid	Mediterranean	Semi-arid	Arid	
RMSE	GG3	GG7	GG22	GG22	GG20	GG20	GG22
BIAS	GG1	GG7	GG20	GG22	GG14	GG14	GG18
$R^2$	GG17 & GG23	GG11 & GG13	GG18 & GG20	GG18 & GG20	GG17 & GG23	GG18 & GG20	GG18 & GG20

[Title Page](#)
[Abstract](#)
[Introduction](#)
[Conclusions](#)
[References](#)
[Tables](#)
[Figures](#)
[⏪](#)
[⏩](#)
[◀](#)
[▶](#)
[Back](#)
[Close](#)
[Full Screen / Esc](#)
[Printer-friendly Version](#)
[Interactive Discussion](#)

## A universal evapotranspiration model

F. M. Anayah and  
J. J. Kaluarachchi

**Table 6.** Comparison of performance of GG18 model to the most recently published ET studies.

Citation	Method	# of sites	RMSE (mm month <sup>-1</sup> )			BIAS (mm month <sup>-1</sup> )			R <sup>2</sup>		
			min	max	mean	min	max	mean	min	max	mean
Present study	GG18 model	34	10.3	59.9	20.6	0.5	58.1	10.6	0.01	0.94	0.64
Suleiman and Crago (2004)	Radiometric surface temperature	2	32.0	53.4					0.78	0.94	
Mu et al. (2007)	Revised remote sensing and Penman–Monteith	19	7.7	56.4	29.2	2.9	41.1	15.6	0.13	0.96	0.76
Szilagyi and Kovacs (2010)	CRAE	3	2.6	39.7	15.3	0.0	21.0	8.4	0.79	0.95	0.85
Han et al. (2011)	Enhanced GG	4	3.7	16.0	10.7				0.82	0.98	0.92
Huntington et al. (2011)	Modified AA	5			11.0						0.71
Mu et al. (2011)	Modified remote sensing and Penman–Monteith	46	9.4	52.0	25.6	0.3	28.6	10.0	0.02	0.93	0.65
Thompson et al. (2011)	Penman–Monteith and soil moisture	14	34.0	175.0	94.1						

[Title Page](#)
[Abstract](#)
[Introduction](#)
[Conclusions](#)
[References](#)
[Tables](#)
[Figures](#)
[Back](#)
[Close](#)
[Full Screen / Esc](#)
[Printer-friendly Version](#)
[Interactive Discussion](#)

## A universal evapotranspiration model

F. M. Anayah and  
J. J. Kaluarachchi

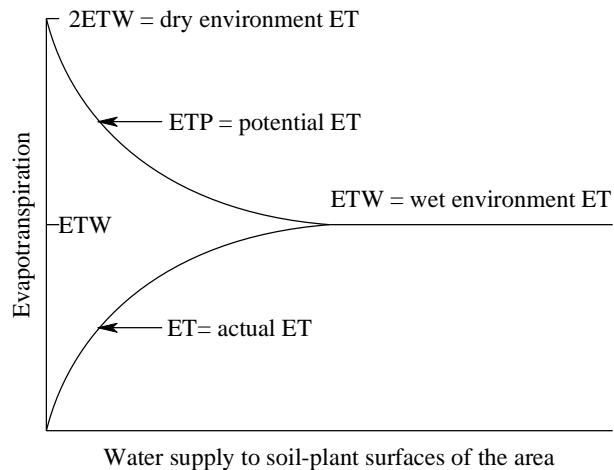


**Fig. 1.** A schematic representation of the complementary relationship between ET, ETW and ETP (after Morton, 1983).

[Title Page](#)[Abstract](#)[Introduction](#)[Conclusions](#)[References](#)[Tables](#)[Figures](#)[⏪](#)[⏩](#)[◀](#)[▶](#)[Back](#)[Close](#)[Full Screen / Esc](#)[Printer-friendly Version](#)[Interactive Discussion](#)

# HESSD

10, 13595–13634, 2013

## A universal evapotranspiration model

F. M. Anayah and  
J. J. Kaluarachchi

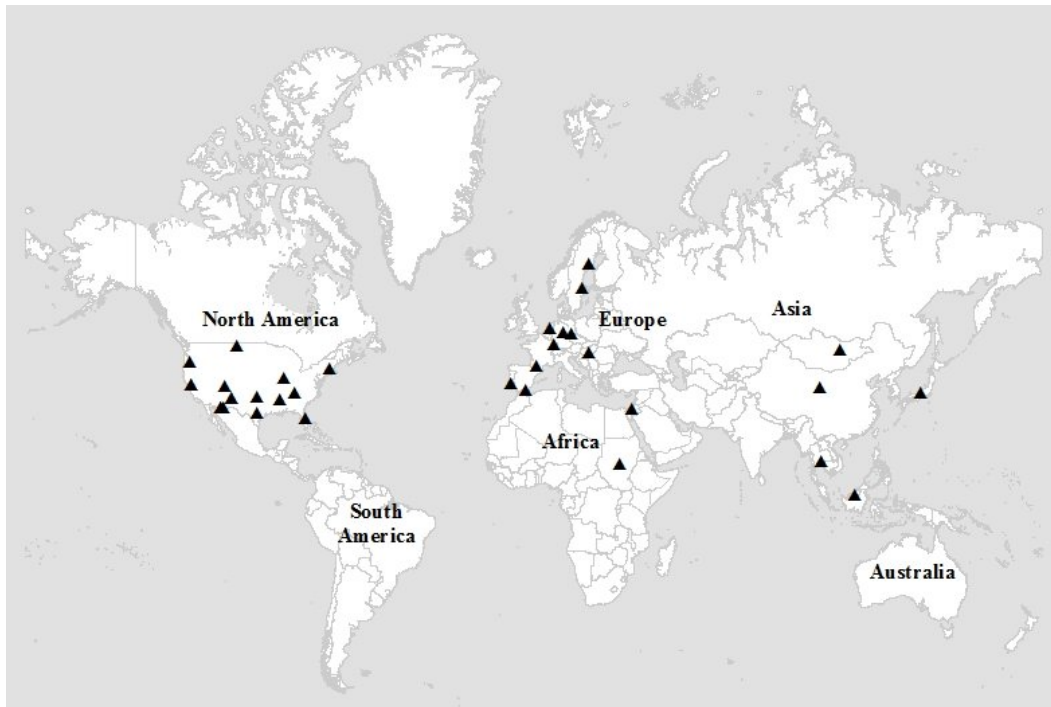


**Fig. 2.** Map showing the locations of the 34 EC sites with measured ET flux data.

[Title Page](#)[Abstract](#)[Introduction](#)[Conclusions](#)[References](#)[Tables](#)[Figures](#)[|◀](#)[▶|](#)[◀](#)[▶](#)[Back](#)[Close](#)[Full Screen / Esc](#)[Printer-friendly Version](#)[Interactive Discussion](#)

## A universal evapotranspiration model

F. M. Anayah and  
J. J. Kaluarachchi

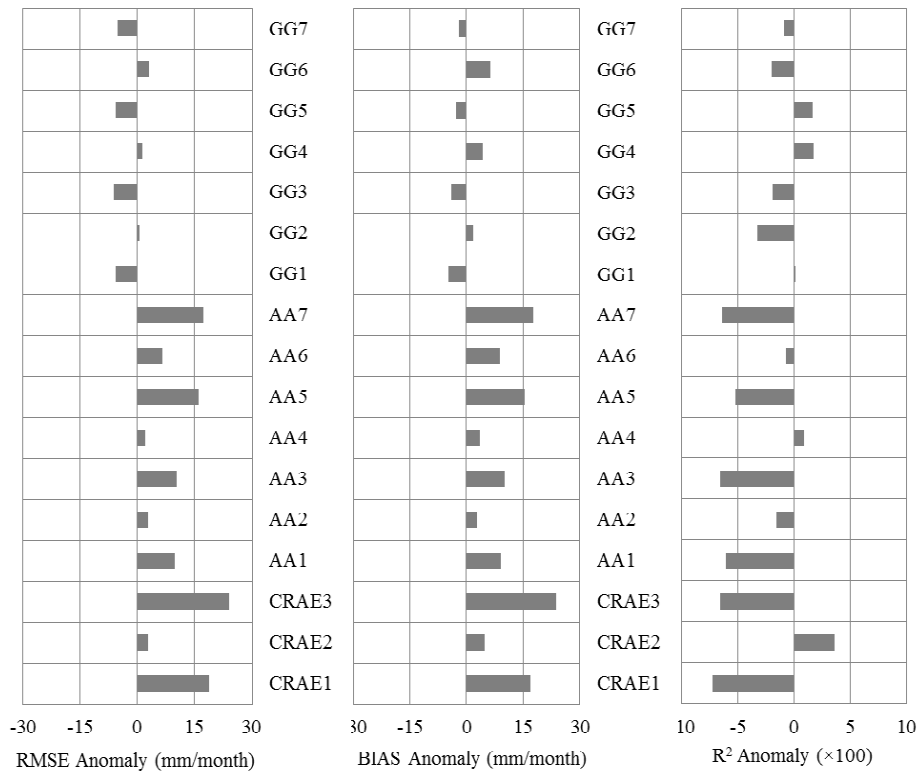


**Fig. 3.** Anomalies of RMSE, BIAS and  $R^2$  values for 17 model variations across the 34 sites. Here anomalies are computed based on the values computed with each corresponding complementary method.

[Title Page](#)  
[Abstract](#)   [Introduction](#)  
[Conclusions](#)   [References](#)  
[Tables](#)   [Figures](#)  
⏪   ⏩  
◀   ▶  
[Back](#)   [Close](#)  
[Full Screen / Esc](#)  
[Printer-friendly Version](#)  
[Interactive Discussion](#)



## A universal evapotranspiration model

F. M. Anayah and  
J. J. Kaluarachchi

Title Page

Abstract

Introduction

Conclusions

References

Tables

Figures

◀

▶

◀

▶

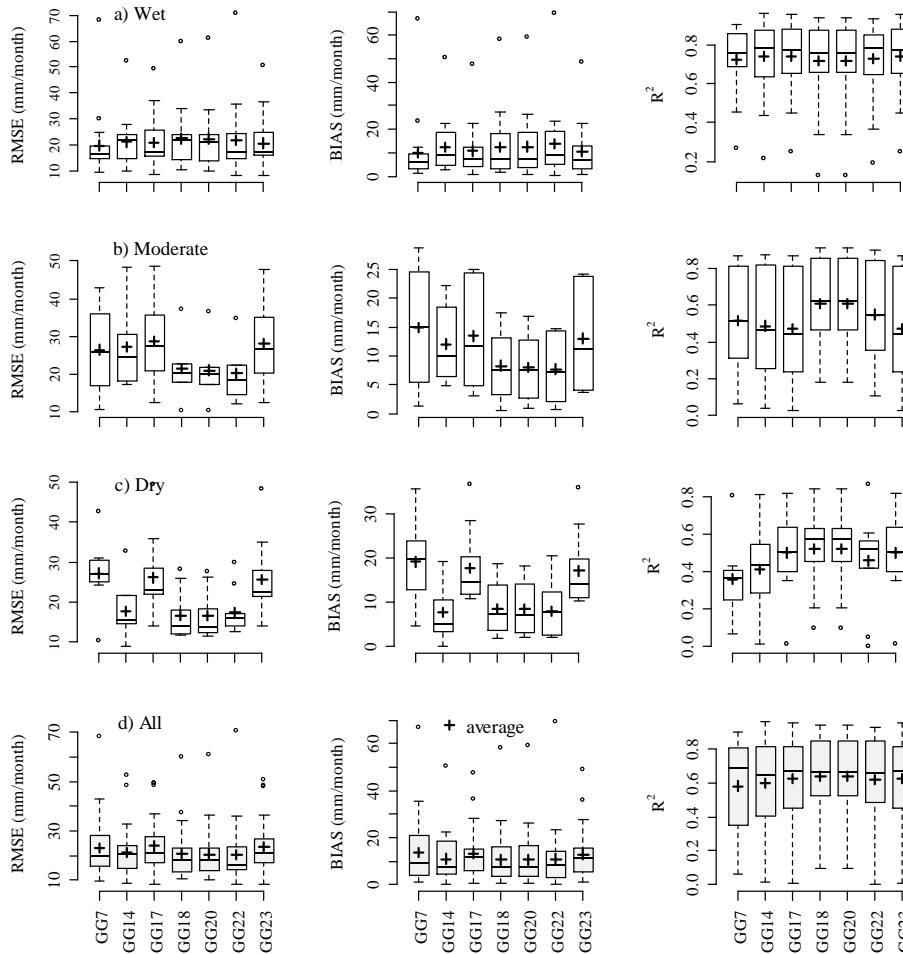
Back

Close

Full Screen / Esc

Printer-friendly Version

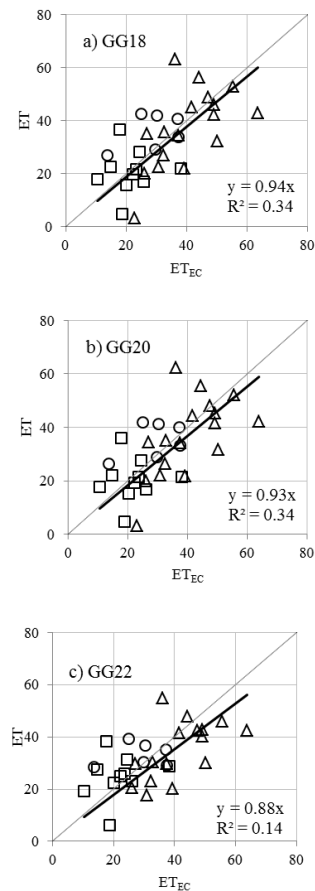
Interactive Discussion



**Fig. 4.** Boxplots of RMSE, BIAS and  $R^2$  metrics of the seven promising model variations for the simplified climatic classes.

## A universal evapotranspiration model

F. M. Anayah and  
J. J. Kaluarachchi

[Title Page](#)[Abstract](#)[Introduction](#)[Conclusions](#)[References](#)[Tables](#)[Figures](#)[⏪](#)[⏩](#)[◀](#)[▶](#)[Back](#)[Close](#)[Full Screen / Esc](#)[Printer-friendly Version](#)[Interactive Discussion](#)

**Fig. 5.** Scatter plots of average ET estimates ( $\text{mm month}^{-1}$ ) for GG18, GG20 and GG22 model variations in comparison to measured  $\text{ET}_{\text{EC}}$  fluxes from 33 sites (all except site 4) in the wet (triangle), moderate (circle) and dry (square) climatic classes.

## A universal evapotranspiration model

F. M. Anayah and  
J. J. Kaluarachchi

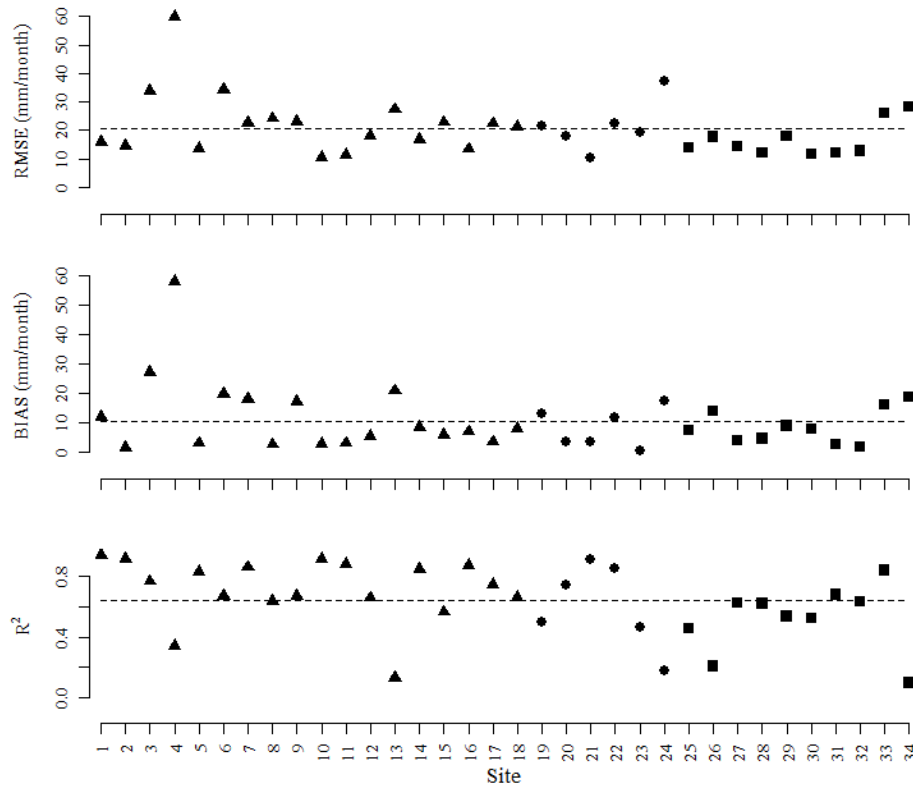


**Fig. 6.** RMSE, BIAS and  $R^2$  of the GG18 model variation at each site in the wet (triangle), moderate (circle) and dry (square) climatic classes and the dashed lines indicate the average values.

[Title Page](#)
[Abstract](#)
[Introduction](#)
[Conclusions](#)
[References](#)
[Tables](#)
[Figures](#)
[⏪](#)
[⏩](#)
[⏴](#)
[⏵](#)
[Back](#)
[Close](#)
[Full Screen / Esc](#)
[Printer-friendly Version](#)
[Interactive Discussion](#)

# HESSD

10, 13595–13634, 2013

## A universal evapotranspiration model

F. M. Anayah and  
J. J. Kaluarachchi

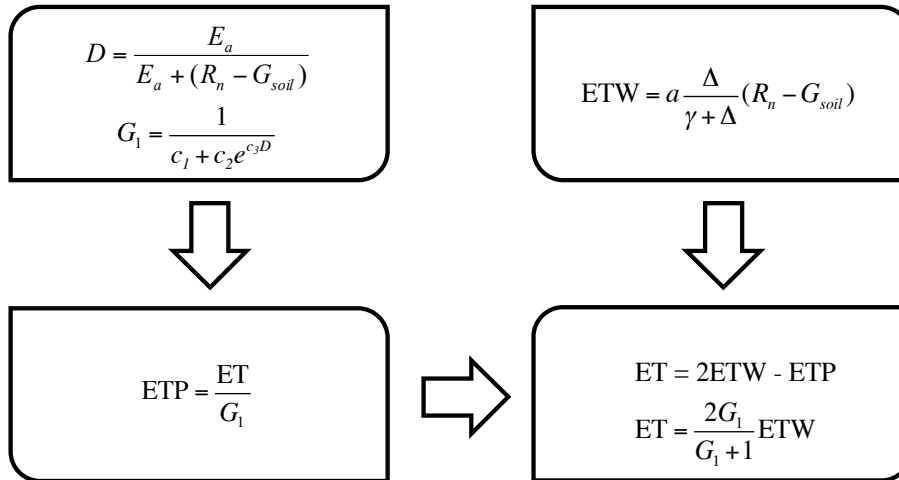


Fig. 7. Schematic showing the structure of the proposed GG18 model.

Title Page	
Abstract	Introduction
Conclusions	References
Tables	Figures
◀	▶
◀	▶
Back	Close
Full Screen / Esc	
Printer-friendly Version	
Interactive Discussion	

